Nuclear Instruments and Methods in Physics Research A ∎ (∎∎∎∎) ∎∎∎–∎∎∎

Contents lists available at ScienceDirect

Nuclear Instruments and Methods in Physics Research A

journal homepage: www.elsevier.com/locate/nima

Acceleration of electrons under the action of petawatt-class laser pulses onto foam targets

L.P. Pugachev [a,*], N.E. Andreev [a], P.R. Levashov [a], O.N. Rosmej [b]

[a] Joint Institute for High Temperatures of the Russian Academy of Sciences, Izhorskaya 13 Bldg 2, 125412 Moscow, Russia
[b] GSI Helmholtzzentrum für Schwerionenforschung GmbH, Planckstraße 1, 64291 Darmstadt, Germany

ARTICLE INFO

Article history:
Received 1 December 2015
Received in revised form
27 January 2016
Accepted 18 February 2016

Keywords:
Laser–plasma interaction
Acceleration of electrons
Petawatt-class laser pulses
Foam targets
Relativistic self-focusing and channeling

ABSTRACT

Optimization study for future experiments on interaction of petawatt laser pulses with foam targets was done by 3D PIC simulations. Densities in the range $0.5n_c$–n_c and thicknesses in the range 100–500 μm of the targets were considered corresponding to those which are currently available. It is shown that heating of electrons mainly occurs under the action of the ponderomotive force of a laser pulse in which amplitude increases up to three times because of self-focusing effect in underdense plasma. Accelerated electrons gain additional energy directly from the high-frequency laser field at the betatron resonance in the emerging plasma density channels. For thicker targets a higher number of electrons with higher energies are obtained. The narrowing of the angular distribution of electrons for thicker targets is explained by acceleration in multiple narrow filaments. Obtained energies of accelerated electrons can be approximated by Maxwell distribution with the temperature 8.5 MeV. The charge carried by electrons with energies higher than 30 MeV is about 30 nC, that is 3–4 order of magnitude higher than the charge predicted by the ponderomotive scaling for the incident laser amplitude.

1. Introduction

A number of theoretical studies [1–8] on the interaction of relativistic picosecond laser pulses with near-critical few mm scale plasma were carried out. Most of them [1–4,6] were motivated by the fast ignition scheme for the inertial confinement fusion [9]. Other works [7,8] are motivated by applications concerned with X-ray generation [10] and ion acceleration from a target with pre-plasma. For the fast ignition scenario it is necessary to deliver a laser pulse through preplasma at a target critical surface with minimal losses. The main emphasis in the works [3,4,6] is made on efficient transmission of petawatt laser pulses in plasma. At these parameters a number of highly nonlinear processes take place such as self-focusing, wakefield [11] and quasistatic fields' generation [1,2], filamentation, filament coalescence [12,3,6], hosing [13,3,6], surface waves [13,4,5,14], parametric instabilities. Mechanisms of electron acceleration were considered in detail in the works [1,2,5,7]. It was shown [1,2] that electrons can gain energy directly from the laser field performing betatron oscillations inside density channels. Besides, parametric amplification of betatron oscillations [7] and acceleration in surface waves near the channel walls [5] can take place. The stable channeling and transmission of picosecond laser pulses in near-critical density plasma were studied experimentally [15–18]. The experiments [19–21] confirm generation of electron bunches which cannot be explained by the only wakefield production.

Low density foam is a very prospective material for the construction of secondary electron and X-ray sources intended to diagnose matter in high energy density (HED) states which can be obtained via volumetric heating of macroscopic samples of high Z elements by means of intense heavy ion beams [22,23]. Such experiments will offer unique opportunities for dense plasma research on the macroscopic scale in conditions close to thermodynamic equilibrium. In order to radiograph macroscopic with the areal density of the order of a few g/cm^2 (e.g. 1 mm lead at solid density), 100 keV gamma-rays or tens of MeV energetic electrons are required. High absorption properties of HED-samples and an extreme environment caused by the parasitic radiation induced in intense heavy ion beam–target interaction define requirements on strong increase of the electron/gamma-ray beam fluence at high energies. The results of this paper based on 3D PIC simulations demonstrate that interaction of the relativistic laser pulse with near critical plasma layer leads to effective generation of highly energetic electrons of tens of MeV energy carrying the charge that many orders of magnitude exceed the value predicted by the ponderomotive scaling for the incident laser amplitude.

The laser parameters correspond to those which can be obtained at the PHELIX laser system GSI, Darmstadt and the target

* Corresponding author.
E-mail address: pulleon@mail.ru (L.P. Pugachev).

http://dx.doi.org/10.1016/j.nima.2016.02.053

thicknesses are in the range 100–500 μm. Electron acceleration mechanisms are analyzed relevant to these laser-plasma parameters. Until recently PIC modelling was performed in 2D spatial geometry which cannot describe the processes of self-focusing, self-chanelling and filamentation correctly. Besides, in 2D simulations it is difficult to obtain a correct quantitative description of the electron and ion acceleration processes and to determine charges of the bunches. The emphasis in this work is set on the quantitative optimization of the output electron bunches.

2. Physical and numerical parameters

Simulations in this work were carried out with a 3D PIC code VLPL [24]. A laser pulse has gaussian temporal and transversal shapes. The transversal full width at half maximum (FWHM) $d_{FWHM} = 25$ μm and the temporal FWHM of the pulse $\tau_{FWHM} = 400$ fs. The central laser wavelength equals 1 μm and its intensity is 4×10^{19} W/cm^2 that corresponds to the dimensionless amplitude $a = 5.4$. The pulse is linearly polarized along the y-axis and propagates along the x-axis. The scheme of normal incidence is studied in the work. We consider plasma layers with three different thicknesses l of 100, 300 and 500 μm and with the electron density $n = 0.5n_c$, where the critical density $n_c = m\omega^2/(4\pi e^2)$, m is the electron mass, ω is the laser frequency, e is the absolute value of the electron charge. Simulations were conducted also with the density $n = n_c$ and the thickness of 100 μm. The plasma is composed of electrons, fully ionized ions of carbon, hydrogen and oxygen. Ions are taken in proportion 3:4:2 which corresponds to the composition of triacetatecellulose $C_{12}H_{16}O_8$ [25,26]. The CHO-polymer foam structure is a 3D regular network with open cells of a micrometer size and 100 nm wall thickness. Foam layers of this material with thicknesses in the range 100–1000 μm and 2 mg/cm^3 volume density are already available for fabrication and have been already used in experiments with intense lasers and heavy ion beams [25–27].

Heating and ionization of the foam material under the action of the prepulse of the laser system are not considered in the simulations. In experiments, fully ionized CHO plasma layers, hydrodynamically stable over ns time scale, can be created via direct irradiation of low density foam with a nanosecond laser prepulse of a moderate intensity (few 10^{14} W/cm^2). In this case, ionization is governed by the supersonic ionization waves, described in [28,29]. Laser intensity, foam density and foam thickness can be matched in such way, that the velocity of the ionization front will be much faster than the ion acoustic velocity and after propagation of the supersonic ionization wave through the target the plasma layer does not undergo notable expansion [28].

A simulation box has a size of 210, 410 or 610 μm along the x-axis depending on the plasma layer thickness. The first 10 and the last 100 μm of the space in this direction are free of the plasma at the initial moment for all simulations. Additional space behind the target is added to determine correctly the amount of electrons which leaves the target completely and forms the electron bunch. The electrons emerging from the target with insufficient energies can return back in the target in the simulations. The box is 100 μm both along the y-axis and the z-axis in all the simulations. The sizes of a numerical cell are 0.05 μm along the x-axis and 0.5 μm along the y-axis and the z-axis. The number of particles per cell equals 4 for the electrons and 1 for the ions of each type. The boundary conditions are absorbing for particles and fields in each direction. At the initial moment the laser pulse is far away from the target and does not affect it. Time is counted from the moment when the center of the laser pulse is at $(x, y, z) = (0, 0, 0)$.

3. Results

The density, the current density and the fields' distributions during propagation of the laser pulse through the target with the thickness $l = 100$ μm and with the initial density $n = 0.5n_c$ are presented in Fig. 1. The plasma initially occupies the region from 10 μm to 110 μm along the x-axis. The density of electrons shown in Fig. 1a exhibits the initial stage of channel formation. This behavior is explained by the relativistic self-focusing of the laser pulse since the critical power $P_c = 17(\omega/\omega_p)^2$ (GW) is exceeded by four orders of magnitude. The formation of the channel with the conical shape is explained by the self-focusing of the pulse during its gradual propagation through the target. The channel expands in the radial direction with the ion sound velocity and the channel radius is visibly changed on timescales $ct \sim 300$ μm. It is seen in Fig. 1b that the laser amplitude of the laser radiation increases in

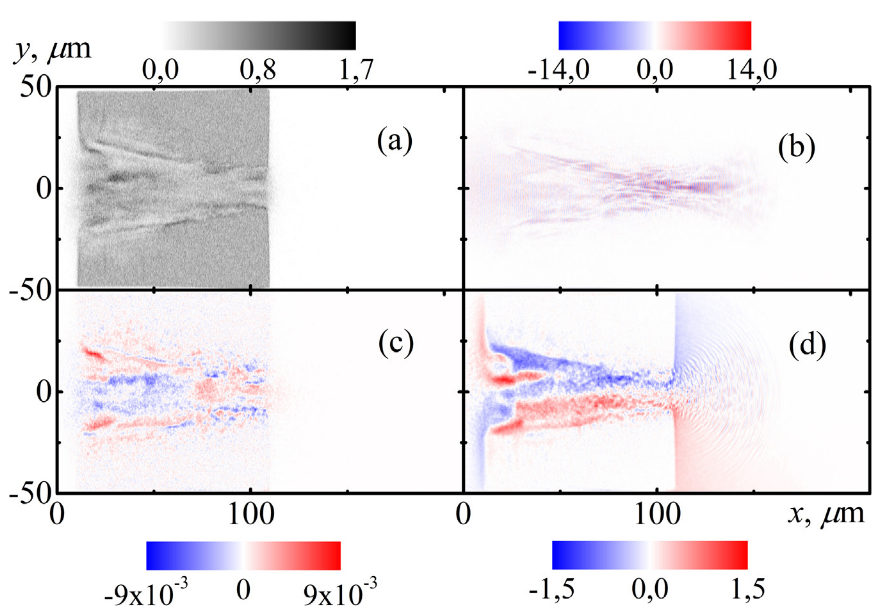

Fig. 1. Simulation with the target thickness $l = 100$ μm at $ct = 100$ μm. The plasma initially occupies the region from 10 μm to 110 μm along the x-axis. Distributions in the plane z=0: (a) electron density, (b) electric field e_y, (c) averaged over the laser period current density $\langle j_x \rangle$, (d) averaged over the laser period magnetic field $\langle b_z \rangle$.

Please cite this article as: L.P. Pugachev, et al., Nuclear Instruments & Methods in Physics Research A (2016), http://dx.doi.org/10.1016/j.nima.2016.02.053